

Andreev drag effect via magnetic quasiparticle focusing in normal-superconductor nanojunctions

P. K. Polinák,¹ C. J. Lambert,¹ J. Koltai,² and J. Cserti³

¹*Department of Physics, Lancaster University, Lancaster, LA1 4YB, United Kingdom*

²*Department of Biological Physics, Eötvös University, H-1117 Budapest, Pázmány Péter sétány 1/A, Hungary*

³*Department of Physics of Complex Systems, Eötvös University, H-1117 Budapest, Pázmány Péter sétány 1/A, Hungary*

(Received 22 August 2006; published 27 October 2006)

We study a hybrid normal-superconductor (NS) π junction in which the nonlocal current can be orders of magnitude larger than that in earlier proposed systems. We calculate the electronic transport of this NS hybrid system when an external magnetic field is applied. It is shown that the nonlocal current exhibits oscillations as a function of the magnetic field, making the effect tunable with the field. The underlying classical dynamics is qualitatively discussed.

DOI: 10.1103/PhysRevB.74.132508

PACS number(s): 74.45.+c, 75.47.Jn

Electron-transport properties of normal-superconductor hybrid nanostructures have been the subject of extensive theoretical and experimental¹ attention. Experiments carried out on nanostructures containing ferromagnets (F) and superconductors (S) reveal novel features, not present in normal-metal/superconductor (NS) junctions, due to the suppression of electron-hole correlations in the ferromagnet. When spin-flip processes are absent, further effects are predicted, including the suppression of conventional giant magnetoresistance in diffusive magnetic multilayers² and the appearance of nonlocal currents when two fully polarized ferromagnetic wires with opposite polarizations make contact with a spin-singlet superconductor.^{3,4} The latter effect, also called the Andreev drag effect, has been highlighted, because of interest in the possibility of generating entangled pairs of electrons at an NS interface.⁵ A recent study of such a junction in the tunneling limit³ predicts that the magnitude of the nonlocal current decreases exponentially as $\exp(-2L/\pi\xi_c)$, where ξ_c is the superconducting coherence length, and L is the distance between the F contacts. The effect can be enhanced by inserting a diffusive normal conductor between the superconductor and the ferromagnetic contacts leads as shown in Refs. 6 and 7. The off-diagonal conductance,³ which is always negative in the normal case, can have a positive value of order the contact conductances of these systems. However, the value of the off-diagonal conductance is determined by fixed material parameters, such as the polarization of the ferromagnets, and the spin-flip time in the normal diffusive conductor. Therefore, it is of interest to study alternative methods for material-independent tuning of the nonlocal current.

In this work, we show that even in the absence of ferromagnetic contacts, an enhanced Andreev drag effect is possible with the NS structure shown in Fig. 1. We shall demonstrate that the nonlocal current is enhanced by orders of magnitude compared with the structure in which ferromagnetic leads were used to detect the current.³ Moreover, the magnitude of the nonlocal current can be tuned by varying a magnetic field applied perpendicular to the system. The necessary field is much lower than the critical field of the superconductor.

In double-point-contact electron-focusing experiments the same geometry shown in Fig. 1 was used by Tsoi *et al.* to observe directly, for the first time, the Andreev reflection.⁸ Independently, similar experiments by Benistant *et al.* were

performed,^{9,10} and they found γ dips (see Fig. 2 in Ref. 9) in the measurement of the field-dependent voltage at the collector which were interpreted semiclassically. In this work, we present a full quantum calculation to investigate these γ dips. Our semiclassical consideration is an extension of that in Ref. 9 by taking into account the finite width W_N of the waveguide. We find a good agreement between the quantum and the semiclassical calculations.

To calculate the nonlocal current we employ the current-voltage relation developed for normal/superconducting hybrid structures in the linear response limit.¹¹ Assuming that the voltage v_2 at lead 2 is the same as the voltage v of the condensate potential, for the arrangement shown in Fig. 1 one finds that the currents in lead 1 and 2 are

$$I_1 = \frac{2e^2}{h}(N - R_0 + R_a)(v_1 - v), \quad (1a)$$

$$I_2 = \frac{2e^2}{h}(T_a - T_0)(v_1 - v), \quad (1b)$$

where v_1 is the voltage at lead 1 and N is the number of open scattering channels in the normal leads of width W_L . Here R_0 (T_0) are the reflection (transmission) coefficients for an electron from lead 1 to be reflected (transmitted) to lead 1 (2),

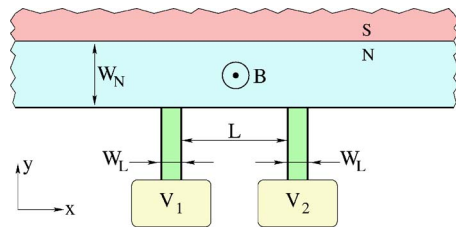


FIG. 1. (Color online) The hybrid NS nanostructure consists of an infinitely long NS ballistic waveguide, comprising a normal metal (N) of width W_N coupled to a spin-singlet superconductor (S) region of a width that is much larger than the superconducting coherence length ξ_c . To measure the nonlocal current, two ballistic normal leads (emitter and collector), at voltages v_1 and v_2 , and with width W_L , separated by a distance L , are in contact with the normal waveguide. The left and right ends of the waveguide act as drains which absorb any quasiparticles exiting to the left or right. The magnetic field B is applied perpendicular to the system (in our calculation $B > 0$ corresponds to a field pointing out of the plane of the system).

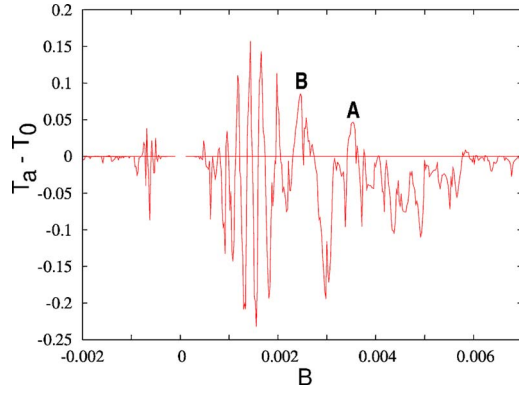


FIG. 2. (Color online) $T_a - T_0$ as a function of the magnetic field [in units of $\Phi_0/(2a^2\pi)$] at the Fermi energy E_F . In lead 1 only one mode was allowed. The wave functions at magnetic fields corresponding to letters A and B on the peaks of the curves will be shown in Fig. 5.

and R_a (T_a) are the Andreev reflection (transmission) coefficients for an electron from lead 1 to be reflected (transmitted) to lead 1 (2) as a hole. R_a and R_0 satisfy the inequality $N - R_0 + R_a \geq 0$; thus, I_1 is always positive for positive $v_1 - v$. All coefficients are evaluated at the Fermi energy using an exact scattering matrix formalism.

It is easy to see from Eq. (1) that whenever Andreev transmission dominates normal transmission (i.e., $T_a > T_0$) the currents I_1 and I_2 have the same signs, i.e., a current in lead 1 induces a current in lead 2 flowing in the same direction. In the semiclassical point of view, this means that holelike quasiparticles leave the system at lead 2. This is the Andreev drag effect. On the other hand, in the case when the normal transmission is larger than the Andreev transmission (i.e., $T_a < T_0$), electronlike quasiparticles leave the system through lead 2, yielding a current flowing opposite to the direction of the current in lead 1.

In what follows now, we show that for the system depicted in Fig. 1 the ratio T_a/T_0 can be tuned by an applied magnetic field. To this end, we calculate the transmission coefficients for the system using the Green's function technique¹² developed for a discrete lattice. Each site is labeled by discrete lattice coordinates (x, y) and possesses particle (hole) degrees of freedom $\psi^{(h)}(x, y)$. The magnetic field is incorporated via a Peierls substitution. In the presence of local s -wave pairing described by a superconducting order parameter $\Delta(x, y)$, the Bogoliubov–de Gennes equation¹³ for the retarded Green's function takes the form

$$\begin{pmatrix} \mathbf{H} - E & \Delta \\ \Delta^* & -\mathbf{H}^* + E \end{pmatrix} \begin{pmatrix} G^{ee} & G^{eh} \\ G^{he} & G^{hh} \end{pmatrix} = - \begin{pmatrix} \mathbf{1} & \mathbf{0} \\ \mathbf{0} & \mathbf{1} \end{pmatrix}, \quad (2a)$$

where the components of \mathbf{H} are

$$\begin{aligned} \mathbf{H}_{x,x',y,y'} &= (\epsilon_0 - E_F) \delta_{x,x'} \delta_{y,y'} - \sum_{n_x} \gamma_x \delta_{x+n_x,x'} \delta_{y,y'} \\ &\quad - \sum_{n_y} \gamma_y \delta_{x,x'} \delta_{y+n_y,y'}. \end{aligned} \quad (2b)$$

Here E_F is the Fermi energy, and n_x and n_y are the nearest neighbors of (x, y) in the x and y direction, respectively.

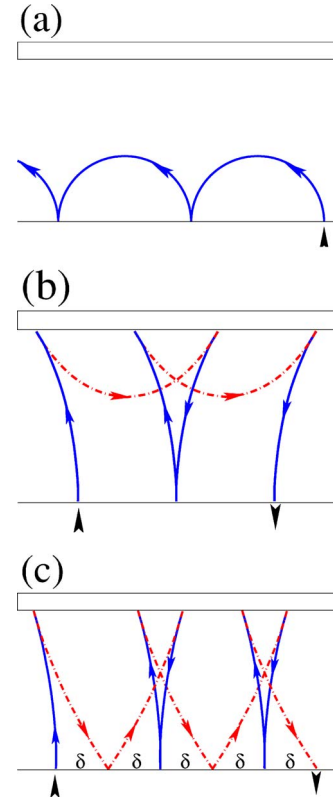


FIG. 3. (Color online) Classical trajectories in a magnetic field. (a) shows the case when the electron does not reach the NS interface. New types of trajectories involving Andreev reflections are sketched in (b) and (c), for the cases when only the electron (b) or both the electron and the hole (c) can reach the side of the waveguide where the leads are attached. Solid blue (dotted-dashed red) lines refer to the electron (hole). Electrons are injected perpendicularly into the waveguide at the positions marked by arrows pointing up.

Within the Landau gauge with a vector potential in the x direction, $\gamma_x = \gamma_0 e^{i\theta(y)}$, $\gamma_y = \gamma_0$, where γ_0 is the hopping parameter without magnetic field. The phase $\theta(y)$ for the Peierls substitution is zero in the superconducting region, and it is given by $\theta(y) = Ba^2\pi(W_N - y)/\Phi_0$ in the normal region, where a is the lattice constant,¹⁴ and $\Phi_0 = h/2e$ is the flux quantum. This choice of gauge results in a uniform magnetic field B in the normal region, and zero magnetic field in the S region, while the translation invariance in the x direction is preserved. The order parameter is assumed to be a step function,^{15,16} i.e., constant Δ_0 in the S region and zero otherwise. The phase θ is set to $\theta_{\text{lead}} = Ba^2\pi W_N/\Phi_0$ in the leads 1 and 2 to ensure the continuity of the vector potential. The parameters of the Hamiltonian \mathbf{H} are chosen to model an experimentally realizable situation in the quasiclassical regime, i.e., $W_N \gg$ Fermi wavelength.¹⁴

From the Green's function and the scattering matrix for the system, the transmission and reflection coefficients are calculated as a function of the magnetic field. Our central result, shown in Fig. 2, is that the difference between the Andreev and normal transmission coefficients $T_a - T_0$ [which is proportional to the measurable current I_2 according to Eq. (1b)] is an oscillating function of the magnetic field. Furthermore, since positive peaks correspond to a pronounced An-

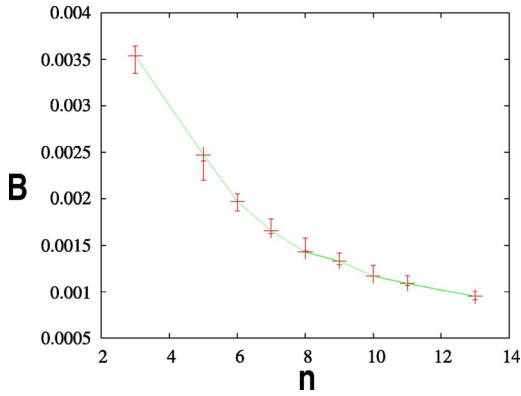


FIG. 4. (Color online) The range of B_n [in units of $\Phi_0/(2a^2\pi)$] shown as a vertical bar for each n , together with those values of magnetic field at which we obtained points in T_a from the quantum transport calculation. (Line connecting these points is only for guiding the eyes.)

dreev drag effect and the heights of the positive peaks are comparable with those of the negative peaks, the nonlocal current can be as large as the normal current in our hybrid system.

A striking feature of Fig. 2 is that it is an asymmetric function of B . This can be understood qualitatively by tracing the classical cyclotron orbits of quasiparticles, bearing in mind that when electron-hole conversion occurs at the NS boundary, the chirality of the electronlike and holelike orbits is preserved and therefore a geometrical construction for their classical trajectories is different from that of normal systems.¹⁷ Examples of trajectories obtained from this geometrical construction are plotted in Fig. 3.

For $B > 0$ electrons injected from lead 1 will follow classical orbits bending to the left. For a large enough $|B|$ these will exit to $x = -\infty$, without reaching the NS interface, and impinging on lead 2, as can be seen in Fig. 3(a). Therefore for large positive B all transmission coefficients from lead 1 to lead 2 vanish. Andreev reflection can occur if $|B|$ is sufficiently small to allow the electrons to reach the NS interface. This condition is defined by $|B| < B_1$, where B_1 is the field for which the cyclotron radius $R_c = W_N$, where $R_c = \sqrt{2mE_F}/eB$. As shown in Figs. 3(b) and 3(c), the transport direction is reversed compared to the normal case due to Andreev scattering, because even if the classical orbits are counterclockwise, quasiparticle transport is to the right, resulting in quasiparticles impinging on lead 2. This is why the asymmetry in Fig. 2 arises. On the other hand, as shown in Fig. 3(b), if R_c is not sufficiently large, there is no drag effect, because the trajectories of the holes do not hit the side of the waveguide to which the leads are attached.

The Andreev drag effect occurs only for $|B| < B_{\max}$, where the maximum field B_{\max} is determined from the condition $R_c \geq 2W_N$. By appropriate choice of the width W_N of the normal part of the waveguide, B_{\max} can be much less than the critical field of the superconductor. The trajectory relevant for this case is shown in Fig. 3(c). On the normal side of the waveguide, normal quasiparticle reflections alternate between electrons and holes, separated by equal distances δ . Assuming that the electrons are injected perpendicularly into the waveguide, simple geometrical considerations give the following condition for maxima in T_a :

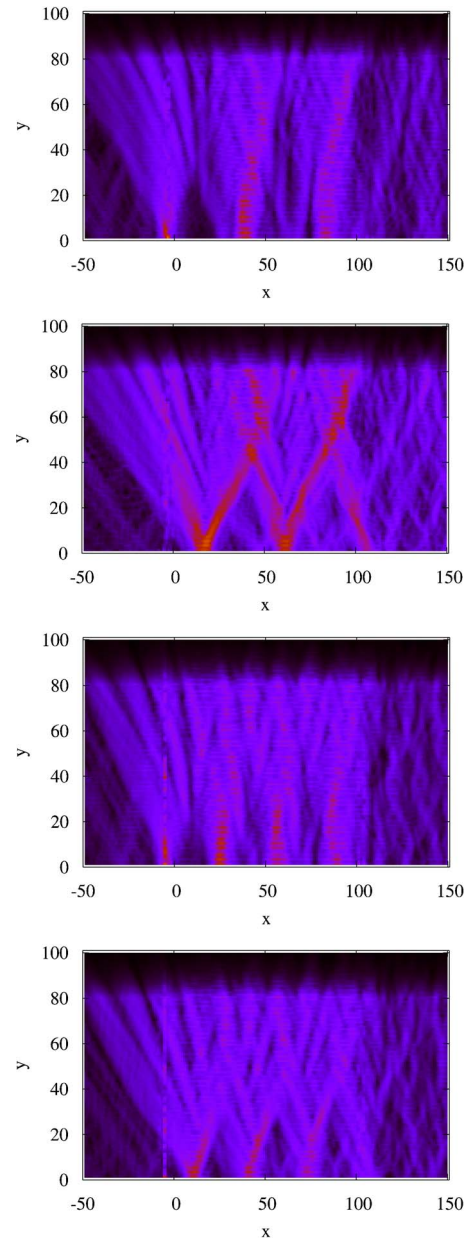


FIG. 5. (Color online) From top to bottom the electron (followed by hole) probability amplitudes are plotted, corresponding to the Andreev-transmission peaks marked by A and B in Fig. 2, respectively. In our geometry $W_N=80$, $W=100$, lead 1 (lead 2) is located at $-10 < x < 0$ ($100 < x < 110$). Distances are in units of the lattice constant (Ref. 14).

$$L = (2n + 1)\delta, \quad (3)$$

where n is an integer counting the number of normal reflections of the hole at the side of the normal waveguide to which the leads are attached, and $\delta = 2\sqrt{R_c^2 - W_N^2} - \sqrt{R_c^2 - 4W_N^2} - R_c$. From Eq. (3) one can find a magnetic field B_n for each n . The peaks in T_a can be expected at B_n . Taking into account the finite widths of the two leads we calculated the ranges of B for each n in which a peak in T_a should be found, which corresponds to the range of B for which a classical trajectory of the hole hits the finite-width interface of lead 2. In Fig. 4 we plotted the ranges of B_n as vertical bars together with

those values of magnetic field at which we obtained peaks from the exact quantum calculations.

One can see that the agreement between the quantum and the classical calculation is reasonable. Thus, this simple classical argument can be used to estimate the magnetic field needed to obtain enhanced Andreev drag.

To reinforce the above detailed classical picture, we now calculate the electron and hole component of the wave functions inside the NS waveguide, and compare them with classical orbits. The contribution of the n th incoming mode (from the left N lead of width W_L) to the wave function at point $\mathbf{r}_S=(x,y)$ of the waveguide is

$$\psi_n^{e(h)}(\mathbf{r}_S) = \sum_{\mathbf{r}_L} G^{ee(he)}(\mathbf{r}_S, \mathbf{r}_L) \chi_n^{+,e}(\mathbf{r}_L), \quad (4)$$

where \mathbf{r}_L runs over the surface of the left lead. Here the appropriate components of the retarded Green's function are defined in Eq. (2a), and $\chi_n^{+,e}(\mathbf{r}_L)$ is the transverse wave function of the n th incoming electron channel of the left lead, normalized to unit flux. The modulus squared of the electron and hole components of the wave function is shown in Fig. 5 for two different magnetic fields, corresponding to the positive peaks A and B in Fig. 2. For these scattering states, the hole probability amplitude has a local maximum at lead 2. There are several other maxima of the probability amplitudes of the wave function at the lower side of the waveguide, both for the holes and for the electrons. For each positive peak of $(T_a - T_0)$, the condition Eq. (3) is satisfied, where n is the number of maxima of the hole probability amplitude be-

tween the leads, and δ is the distance between the nearest electron and hole maxima.

In conclusion, we have shown that even in the absence of ferromagnetic leads, an enhanced nonlocal current can be obtained by including a normal region between the leads and superconductor, and applying magnetic fields perpendicular to the system. The current flowing from lead 1 to lead 2 shows oscillations with alternating signs as a function of magnetic field in the small-field regime, corresponding to alternating magnetic focusing of electron- and holelike quasiparticles between the two leads. Unlike an earlier proposal,³ where T_a is exponentially suppressed with lead separation, the nonlocal current remains significant even for a lead separation much bigger than the coherence length of the superconductor. We discussed how the quantum results could be interpreted qualitatively in a fully classical treatment, providing a better insight into the Andreev drag effect in our system.

For the future it would be of interest to extend the semiclassical approach developed for normal focusing problems. In this analysis one has to involve the classical orbits shown in Fig. 3 in a similar way as in Refs. 17 and 18, and the more complex caustics¹⁹ formed for both electrons and holes.

We would like to thank A. F. Morpurgo, C. W. J. Beenakker, and A. Kormányos for useful discussions. This work is supported by EC Contract No. MRTN-CT-2003-504574, EPSRC, the Hungarian-British TeT, and the Hungarian Science Foundation OTKA Grant No. TO34832.

¹S. K. Upadhyay *et al.*, Phys. Rev. Lett. **81**, 3247 (1998); S. K. Upadhyay *et al.*, Appl. Phys. Lett. **74**, 3881 (1999); R. J. Soulen *et al.*, Science **282**, 85 (1998); C. Fierz *et al.*, J. Phys.: Condens. Matter **2**, 9701 (1990); M. D. Lawrence and N. Giordano, *ibid.* **8**, L563 (1996); V. A. Vasko *et al.*, Phys. Rev. Lett. **78**, 1134 (1997); M. Giroud *et al.*, Phys. Rev. B **58**, R11872 (1998); V. T. Petrashov *et al.*, Phys. Rev. Lett. **83**, 3281 (1999); M. D. Lawrence and N. Giordano, J. Phys.: Condens. Matter **11**, 1089 (1999); F. J. Jedema *et al.*, Phys. Rev. B **60**, 16549 (1999); O. Bourgeois *et al.*, cond-mat/9901045 (unpublished); S. Russo *et al.*, Phys. Rev. Lett. **95**, 027002 (2005).

²F. Taddei *et al.*, Phys. Rev. Lett. **82**, 4938 (1999).

³G. Deutscher and D. Feinberg, Appl. Phys. Lett. **76**, 487 (2000); G. Falci *et al.*, Europhys. Lett. **54**, 255 (2001).

⁴G. Bignon *et al.*, Europhys. Lett. **67**, 110 (2004).

⁵G. B. Lesovik *et al.*, Eur. Phys. J. B **24**, 287 (2001); N. M. Chtchelkatchev *et al.*, Phys. Rev. B **66**, 161320(R) (2002); M. S. Choi *et al.*, *ibid.* **62**, 13569 (2000); R. Mélin, J. Phys.: Condens. Matter **13**, 6445 (2001); P. Recher *et al.*, Phys. Rev. B **63**, 165314 (2001); C. Bena *et al.*, Phys. Rev. Lett. **89**, 037901 (2002); P. Samuelsson *et al.*, *ibid.* **91**, 157002 (2003); New J. Phys. **7**, 176 (2005); E. Prada and F. Sols, Eur. Phys. J. B **40**, 379 (2004); New J. Phys. **7**, 231 (2005).

⁶D. Sánchez *et al.*, Phys. Rev. B **68**, 214501 (2003).

⁷C. J. Lambert *et al.*, in *Towards the Controllable Quantum States*

(*Mesoscopic Superconductivity and Spintronics*), edited by H. Takayanagi and J. Nitta (World Scientific, Singapore, 2003), pp. 119–125 (cond-mat/0310414).

⁸S. I. Bozhko *et al.*, Pis'ma Zh. Eksp. Teor. Fiz. **36**, 123 (1982) [JETP Lett. **36**, 152 (1982)].

⁹P. A. M. Benistant *et al.*, Phys. Rev. Lett. **51**, 817 (1983).

¹⁰P. A. M. Benistant *et al.*, Phys. Rev. B **32**, 3351 (1985).

¹¹C. J. Lambert, J. Phys.: Condens. Matter **3**, 6579 (1991); C. J. Lambert *et al.*, *ibid.* **5**, 4187 (1993); N. K. Allsopp *et al.*, *ibid.* **6**, 10475 (1994); C. J. Lambert and R. Raimondi, *ibid.* **10**, 901 (1998).

¹²S. Sanvito *et al.*, Phys. Rev. B **59**, 11936 (1999).

¹³P. G. de Gennes, *Superconductivity of Metals and Alloys* (Benjamin, New York, 1996).

¹⁴Throughout the paper we set $\gamma=1$, $\epsilon_0=1.5$, $W_N=40a$, and $\Delta_0=0.4$. For having one open channel in the leads 1 and 2 we set $\epsilon_0=3.8$ in the leads of width $W_L=10a$. The Fermi energy is $E_F=4\gamma-\epsilon_0$. The separation between leads is $L=100a$. The lattice constant is $a=(\lambda_F/2\pi)\sqrt{E_F/\gamma}$.

¹⁵W. L. McMillan, Phys. Rev. **175**, 559 (1968); G. Kieselmann, Phys. Rev. B **35**, 6762 (1987).

¹⁶H. Plehn *et al.*, Phys. Rev. B **49**, 12140 (1994).

¹⁷F. Giazotto *et al.*, Phys. Rev. B **72**, 054518 (2005).

¹⁸J. Cserti *et al.*, Phys. Rev. B **69**, 134514 (2004).

¹⁹H. van Houten *et al.*, Phys. Rev. B **39**, 8556 (1989).